

**Bacterial growth through microfiltration membranes and NOM characteristics in an MF-RO integrated membrane system**

**Lab-scale and full-scale studies**

Park, Ji Won; Lee, Young Joo; Meyer, Anne S.; Douterelo, Isabel; Maeng, Sung Kyu

**DOI**

[10.1016/j.watres.2018.07.027](https://doi.org/10.1016/j.watres.2018.07.027)

**Publication date**

2018

**Document Version**

Final published version

**Published in**

Water Research

**Citation (APA)**

Park, J. W., Lee, Y. J., Meyer, A. S., Douterelo, I., & Maeng, S. K. (2018). Bacterial growth through microfiltration membranes and NOM characteristics in an MF-RO integrated membrane system: Lab-scale and full-scale studies. *Water Research*, 144, 36-45. <https://doi.org/10.1016/j.watres.2018.07.027>

**Important note**

To cite this publication, please use the final published version (if applicable).  
Please check the document version above.

**Copyright**

Other than for strictly personal use, it is not permitted to download, forward or distribute the text or part of it, without the consent of the author(s) and/or copyright holder(s), unless the work is under an open content license such as Creative Commons.

**Takedown policy**

Please contact us and provide details if you believe this document breaches copyrights.  
We will remove access to the work immediately and investigate your claim.



# Bacterial growth through microfiltration membranes and NOM characteristics in an MF-RO integrated membrane system: Lab-scale and full-scale studies

Ji Won Park <sup>a</sup>, Young Joo Lee <sup>b</sup>, Anne S. Meyer <sup>c</sup>, Isabel Douterelo <sup>d</sup>, Sung Kyu Maeng <sup>a,\*</sup>

<sup>a</sup> Department of Civil and Environmental Engineering, Sejong University, 209 Neungdong-ro, Gwangjin-gu, Seoul, 05006, Republic of Korea

<sup>b</sup> K-water Convergence Institute, 125 Yuseong-daero 1689 beon-gil, Yuseong-gu, Daejeon, 34045, Republic of Korea

<sup>c</sup> Department of Bionanoscience, Kavli Institute of Nanoscience, Delft University of Technology, Delft, the Netherlands

<sup>d</sup> Pennine Water Group, Department of Civil and Structural Engineering, The University of Sheffield, Sheffield, United Kingdom

## ARTICLE INFO

### Article history:

Received 15 April 2018

Received in revised form

7 July 2018

Accepted 10 July 2018

Available online 11 July 2018

### Keywords:

Biofouling  
Filterable bacteria  
Microfiltration  
NOM  
Reverse osmosis

## ABSTRACT

Biofilm formation on membrane surfaces causes many operational problems such as a decrease in permeate flux and an increase in hydraulic resistance. In this study, the ability of bacteria to pass through microfiltration (MF) membranes and the growth potential of microfilterable bacteria were investigated in order to understand biofouling in MF-reverse osmosis (RO) integrated membrane systems. Growth of microfilterable bacteria in MF permeate was observed, indicating that not all MF membranes can guarantee the total rejection of bacteria. Changes in natural organic matter (NOM) characteristics and growth potential of bacteria during the treatment process are important factors in the occurrence of biofilm development in water treatment systems. Analysis of protein-like and humic-like substances in NOM of two successive RO stages revealed an increase in the concentrations of both biopolymers and humic substances of RO concentrates. Unexpectedly, the use of antiscalants was seen to enhance the growth of bacteria in the RO feed water in this study. Bacterial 16s rRNA pyrosequencing revealed that passing source water through the MF membranes dramatically changed bacterial community structure. The bacterial communities that passed through the MF steps primarily belonged to the family *Comamonadaceae*. However, several bacteria groups including *Flavobacteriaceae*, *Sphingobacteriaceae* and *Sphingomonadaceae* selectively composed the biofilm community formed on the RO membranes. Thus, understanding the selectivity and filterability of MF towards microorganisms involved in biofouling on RO membrane surfaces is crucial for the improvement of membrane-related operational processes.

© 2018 Elsevier Ltd. All rights reserved.

## 1. Introduction

During biofouling, microbial biofilms are formed by the initial attachment of planktonic bacteria to the conditioning layer on membrane surfaces (i.e., seeding effect), followed by the growth of sessile bacteria and the accumulation of extracellular polymeric substances (EPS) such as polysaccharides, proteins, and nucleic acids (Li et al., 2016; Prest et al., 2016). Therefore, the abundance of planktonic bacteria in the source water should be minimized via pretreatment prior to membrane filtration to prevent the formation of biological fouling. Microfiltration (MF) or ultrafiltration (UF) units that are located prior to RO membranes in an integrated

membrane system often play a pretreatment role in separating bacteria and suspended solids from the RO feed water. Thus, integrated membrane systems are often referred to as synergistic techniques because they combine different membrane treatment units.

The growth of microfilterable bacteria (i.e., bacteria that pass through micro-scale filters) can initiate the development of biofilm on subsequent RO membranes. Bacterial communities developed on an RO membrane surface were not affected by MF pretreatment of the RO feed water (Herzberg et al., 2010). Despite previous laboratory-scale MF experiments observed bacterial log removal values (LRVs) ranging above 5 as determined by plate counting, the bacterial load in the water before entering the RO membranes was unacceptable high ( $10^3$ – $10^5$  cells mL<sup>-1</sup> as determined by microscopic counting) (Ghayeni et al., 1999). Considering that

\* Corresponding author.

E-mail address: [smaeng@sejong.ac.kr](mailto:smaeng@sejong.ac.kr) (S.K. Maeng).

cultivation-based methods for detecting microorganisms in water samples typically recover less than 1% of the actual bacterial diversity in the environment, the bacteria that pass through MF in full-scale integrated membrane plants has been traditionally underestimated.

Bacteria are generally reported to be physically larger (range in width from 0.2 to 2  $\mu\text{m}$ ) than MF pores (typically, from 0.1 to 1  $\mu\text{m}$ ), yet the ability of bacteria to pass through MF can be surprisingly high. Filterable bacteria are defined as small cellular forms (0.1–0.3  $\mu\text{m}$ ) of bacteria capable of penetrating through sub-micron sized membrane pores (Wang et al., 2008). Previous studies have verified the presence of 0.1 and 0.2  $\mu\text{m}$  filterable bacteria in various aquatic environments (e.g., seawater, freshwater, and groundwater) (Lillis and Bissonnette, 2001; Wang et al., 2008). Typically, the filterable subfraction of bacteria in oligotrophic freshwater and groundwater consists of less than 10% of total bacteria (Lillis and Bissonnette, 2001; Wang et al., 2009). Several mechanisms of bacterial penetration of an MF membrane pretreatment have been suggested: (1) bacterial motility, (2) bacterial growth and division, and (3) shape-dependent filterability. According to Männik et al. (2009), bacteria can swim through micron channels (e.g., 1.2  $\mu\text{m}$ ) using their own motility. Moreover, bacteria can penetrate sub-micron-width channels by cell shrinkage or division, but not motility. Wang et al. (2008) and Onyango et al. (2010) reported that the bacterial morphologies (e.g., spiral and spherical shaped, respectively) of specific taxa influenced their filterability through submicron filters. In addition, low-nutrient conditions also could reduce bacterial sizes (Lee et al., 2010; Fedotova et al., 2012). Owing to the ability to pass through MF membranes, microfilterable bacteria are often highlighted when testing standard porosity membrane filters (Wang et al., 2008) but are rarely dealt with in industrial applications (Ghayeni et al., 1999; Wang et al., 2008). Therefore, it is important to investigate the growth ability of microfilterable bacteria, which play a crucial role in bacterial passage through MF and in the subsequent development of biofouling on RO membranes.

In addition to the presence of bacteria, biodegradable natural organic matter (NOM) in feed water can also be a precursor to biofilm development on RO membranes. Among the NOM components, assimilable organic carbon (AOC) generally represents the easily biodegradable subfractions of NOM that can be readily assimilated into biomass (i.e., cells). AOC measurement is widely used for predicting the bacterial regrowth and/or potential for biofilm development on the water-contacting surfaces of a variety of materials (e.g., membranes and pipelines) (Hijnen et al., 2009; Nguyen et al., 2012; Prest et al., 2016). Low molecular weight (MW) AOC cannot be completely removed by membrane filtration techniques (e.g., MF and UF) (Escobar and Randall, 2001; Prest et al., 2016). Hijnen et al. (2009) suggested that AOC concentrations in feed water should be lower than 1  $\mu\text{g L}^{-1}$  to prevent biofouling in spiral-wound membranes. This threshold however is difficult to achieve via pretreatments such as membrane filtration (Escobar and Randall, 2001; Prest et al., 2016), considering that reported AOC concentrations in seawater and wastewater treatment plant (WWTP) effluent have been detected at concentrations up to 360 and 420  $\mu\text{g L}^{-1}$ , respectively (Weinrich et al., 2011; Vital et al., 2010). It was recently revealed that the contribution of high MW AOC to bacterial growth is also significant; hence, the characterization of various NOM components, including biopolymers, is important for estimating AOC (Sack et al., 2014; Elhadidy et al., 2016; Park et al., 2016).

The main objective of this study was to investigate the growth potential of filterable bacteria in the integrated membrane system and to characterize the NOM present. With this aim, the effects of integrated membrane system on NOM characteristics, total cell

counts, bacterial adenosine triphosphate (ATP), growth potentials, and bacterial community composition were determined. To overcome the limitations of culturing-based methods, a culture-independent flow cytometry (FCM) application was used to understand bacterial changes (e.g., cell count, membrane permeability, and filterability) during the integrated membrane treatment. In addition, the seeding effect of filterable bacteria on RO membrane biofilms was understood for the first time.

## 2. Materials and methods

### 2.1. Full-scale industrial water treatment plant

A full-scale industrial water treatment plant in Chungcheong province, Korea, was monitored weekly over the course of two months. The surface water was pre-treated via coagulation and sedimentation treatment processes in the Asan drinking water treatment plant (Chungcheong province, Korea) and delivered to the integrated membrane treatment plant (Fig. 1). Source water characteristics were as follows: 6.5–7.5 pH, 221  $\text{mg L}^{-1}$  chloride ions, 978  $\mu\text{S cm}^{-1}$  conductivity, 621  $\text{mg L}^{-1}$  total dissolved solids, 207  $\text{mg L}^{-1}$  total hardness as  $\text{CaCO}_3$ ,  $3.8 \pm 0.5 \text{ mg L}^{-1}$  dissolved organic carbon (DOC), and  $1.6 \pm 0.3 \text{ L mg}^{-1} \text{ m}^{-1}$  specific ultraviolet absorbance at 254 nm ( $\text{SUVA}_{254}$ ). In brief, the integrated

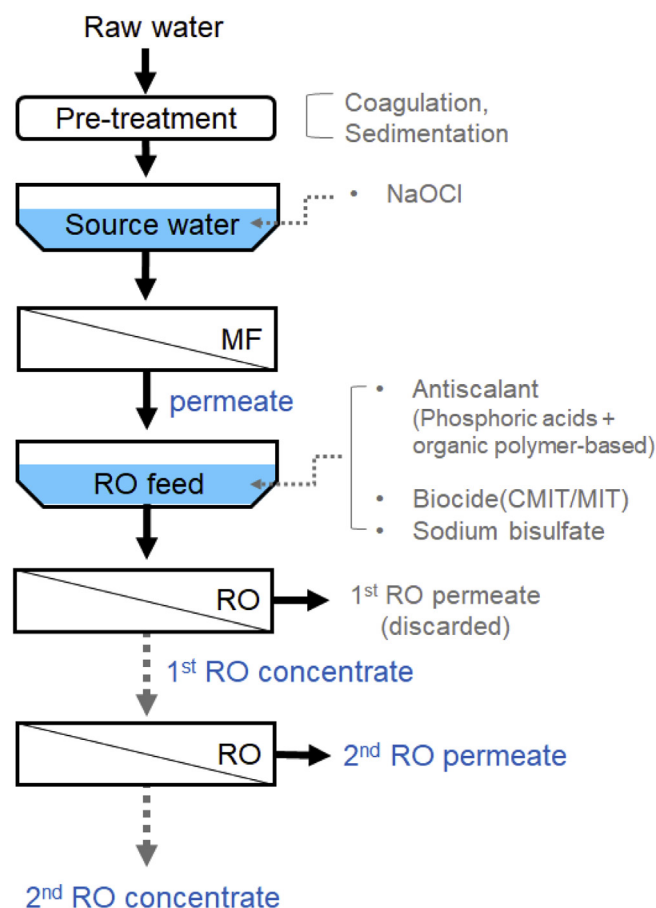


**Fig. 1.** The layout of a monitored full-scale integrated membrane system in this study. Surface water was preliminarily treated by coagulation and sedimentation in a drinking water treatment plant (DWTP), then treated water was delivered and used for the source water. The integrated membrane system consists of microfiltration (MF) and two sequential reverse osmosis (RO) membranes. Source water, MF permeate, RO feed, 1st and 2nd stage RO concentrates, and 2nd stage RO permeate were collected. 1st RO permeate was discarded in this study.

membrane system consisted of a source water basin, MF, RO feed water basin, and 1st and 2nd RO membrane treatment stages (Fig. 1). To control bacteria, 1.5 mg L<sup>-1</sup> of sodium hypochlorite was added to the source water. The MF process consisted of 10 pressurized hollow-fiber MF units (polyvinylidene fluoride, 0.04 μm rated pores, 0.6–1.5 kg cm<sup>-2</sup> of driving pressure, 1.54 m<sup>3</sup> m<sup>-2</sup> day<sup>-1</sup> permeate flux, and 97% recovery rate), which were used to separate bacteria and other particulate substances from the feed water. The MF permeate was delivered to the RO feed water basin (volume 1285 m<sup>3</sup>). The residual free chlorine was quenched by the addition of sodium bisulfate (approximately 2.4 mg L<sup>-1</sup>). Chemicals, including 1 mg L<sup>-1</sup> of antiscalant (phosphoric acid- and organic polymer-based) and 0.5 mg L<sup>-1</sup> of 3:1 mixture of 5-Chloro-2-Methyl-4-Isothiazoline-3-One (CMIT) and 2-Methyl-4-Isothiazoline-3-One (MIT) (i.e., CMIT/MIT), a nonoxidizing biocide, were used to prevent the development of fouling on the polyamide brackish water RO (BWRO) membranes (ESPA2-LD, Hydranautics, USA). Operational details of RO membrane processes are listed in supplementary information (Table S1). Finally, the pH of the RO permeate was adjusted to neutral level, and then the permeate was supplied to local industrial plants, at a volume of approximately 119,000 m<sup>3</sup> per day.

## 2.2. Sample collection from a full-scale treatment plant

We have monitored the full-scale integrated membrane treatment system. Source water and the full-scale treatment plant effluents were collected weekly from the industrial water treatment plant. In total, samples were collected 7 times during the study period ( $n = 7$ ). The samples were analyzed within 5 h of collection. For dissolved NOM characterization, all samples were filtered with a 0.1 μm syringe filter (Sartorius, Germany) and analyzed thereafter. Also, we used both unfiltered and filtered samples to analyze the flow cytometric cell counts and ATP.

## 2.3. Bacterial passage and growth potentials in laboratory test

Integrated membrane system may use various water sources (e.g., wastewater reuse). Since the bacterial properties from surface water and WWTP effluent are significantly different, we simulated the bacterial passage from two water sources; filterable bacteria samples were separated using a 0.1 μm sterile syringe-driven filter (Sartorius, Germany) from the source water of the full-scale plant and Tahnchon WWTP (Seoul, Korea) effluent, respectively. Two indigenous bacteria samples passed through 0.1 μm filters were cultivated at 30 °C for 7 days or more with no nutritional amendment (Wang et al., 2009). We checked the total cell counts and ATP concentrations over the course of 72 h using flow cytometry and ATP assaying, respectively. The growth phases of the bacteria in the MF filtrates were observed over 72 h of cultivation. Two enriched bacteria samples served as inocula for testing the growth potentials of the microfilterable bacteria. Moreover, their bacterial communities were compared to that of the full-scale effluents.

## 2.4. Analysis of NOM characteristics

NOM characteristics were determined through liquid chromatography-organic carbon detection (LC-OCD, Model 8 system, DOC-Labor, Germany) and an excitation-emission matrix (EEM). LC-OCD analysis was used to group DOC into five sub-fractions, namely biopolymers (>20 kDa), humic substances (1–20 kDa), building blocks (<500 Da), low MW acids, and low MW neutrals (<350 Da), arranged in descending order by MW. Information on these sub-fractions has been described in more detail elsewhere (Huber et al., 2011). The change in fluorescent properties

of the DOC was obtained via a 3D-excitation-emission matrix (EEM), using a spectrofluorophotometer (RF-5301PC, Shimadzu, Japan). Fluorescence intensities were recorded in a range of excitation (ex) wavelengths from 220 to 400 nm (10 nm intervals) and emission (em) wavelengths from 280 to 600 nm (1 nm intervals). The fluorescence profiles monitored in this study were T1 (tryptophan-like, ex 220–240 nm, and em 330–360 nm), T2 (tyrosine-like, ex 270–280 nm, and em 330–360 nm), A (fulvic-like, ex 230–260 nm, and em 400–450 nm), and C (humic-like, ex 300–340 nm, and em 400–450 nm) (Park et al., 2016).

## 2.5. Flow cytometry and ATP measurement

Bacterial abundance and viability were measured using SYBR Green I/propidium iodide (PI) staining protocols and a luciferase ATP assay (Vital et al., 2012; Park et al., 2016). The stained cells were recorded using a Partec Cube 6 flow cytometer (Partec GmbH, Germany). The electronic gating and cell count calculation were performed via FCS Express 4 software (De Novo Software, CA, USA). Intact/damaged cell cytograms were electronically gated for cell enumeration according to the method from previous studies (Berney et al., 2008; Park et al., 2016). Intact cell counts were electronically gated into two representative bacterial domains, “low nucleic acid content (LNA)” and “high nucleic acid content (HNA)” for each sample. Intact LNA and HNA bacteria were separated based on their gaps of green fluorescence signals (530 nm). LNA bacteria primarily consist of relatively small, less active and filterable bacteria in environmental water samples (Gasol et al., 1999; Wang et al., 2009), whereas HNA bacteria represent a relatively large and active bacterial subfraction (Gasol et al., 1999; Park et al., 2016).

The growth potentials of microfilterable bacteria were determined via the method presented by Vital et al. (2010). All treatment effluents from the full-scale plant were pasteurized at 70 °C for 30 min and filtered with 0.1 μm syringe filters (Sartorius, Germany). Then, 1.0 × 10<sup>4</sup> cells mL<sup>-1</sup> of each inoculum was introduced to pasteurized water samples. The inoculated samples were cultivated for 48 h at 30 °C in the dark, and then the growth potentials were evaluated. The total cell concentration of the inoculum and grown cell count were obtained using the SYBR Green I staining protocol (Vital et al., 2010; Park et al., 2016).

Bacterial ATP was quantified. In brief, water samples were first filtered with 0.1 μm syringe filters (Sartorius, Germany). Then, 100 μL of each ATP reagent (BacTiter-Glo™, Promega, USA) was added to 100 μL of the filtered (free ATP) and unfiltered (total ATP) water samples, mixed gently, incubated at 36 °C for 1 min, and measured via a GloMax 20/20 Luminometer (Turner BioSystems, USA). Bacterial ATP was determined by subtracting the free ATP from the total ATP (Park et al., 2016).

## 2.6. Bacterial community analysis

The bacterial communities of the syringe-filtered MF permeates and full-scale water samples as well as the RO membrane biofilms were investigated by sequencing the 16s rRNA gene to reveal the fate of the filterable bacteria. DNA was extracted from source water, MF permeate, RO concentrate, RO biofilm, filterable bacteria cultivated from the source water and WWTP effluent samples using a FastDNA SPIN kit (MP Biomedicals, USA). A detailed description of RNA gene sequence is given in the supplemental information. Taxonomical assignment were acquired in family-level (e.g., relative abundance and principal component analysis [PCA]). We have also calculated the Shannon index ( $H'$ ) to compare the changes of bacterial diversity of samples in species-level (Shannon, 1997).

### 3. Results and discussion

#### 3.1. Fate of NOM characteristics in a full-scale integrated membrane system

Changes in NOM characteristics during a treatment process provide crucial information for understanding the rejection efficacy in membrane water systems as well as the growth potential of indigenous bacteria (Park et al., 2016). Previously, only low-MW NOM compounds were highlighted as major AOC components when *Pseudomonas fluorescens* P-17 and *Spirillum* sp. strain NOX were used. However, recent studies reported that high-MW organics, including biopolymers, cannot be underestimated when indigenous bacteria are used for AOC assay (Sack et al., 2014; Elhadidy et al., 2016; Park et al., 2016). In addition, bacteria utilized high MW DOC such as aromatic proteins and/or biopolymers to a greater extent than that of low MW DOC (Nguyen et al., 2012). In order to fully understand the changes in NOM profile during water treatment within a full-scale integrated membrane system, this study has determined the concentrations of each type of NOM sub-component at different stages of the purification process. In the source water of the full-scale integrated membrane system, the DOC concentration was  $3.8 \pm 0.5 \text{ mg L}^{-1}$ , consisting of 2% biopolymers, 33% humic substances, 20% building blocks, 7% low-MW acids, and 38% low-MW neutrals (Fig. 2). Low-MW organic matter fractions (<500 Da) were 65% of the total DOC composition. EEM fluorescence intensities in the T1, T2, A, and C peak regions were  $482 \pm 30$ ,  $245 \pm 14$ ,  $684 \pm 41$ , and  $466 \pm 28$  a.u., respectively (Fig. S1). The DOC constituents of the source water were predominated by fulvic-like substances, which occur naturally in soils and are relatively hydrophilic. In addition, SUVA<sub>254</sub> was  $1.5 \text{ L mg}^{-1} \text{ m}^{-1}$  (data not shown), which is corresponded to a relatively hydrophilic NOM characteristic in freshwater. According to our previous study, NOM characteristics were affected by pretreatment using coagulation/sedimentation (Park et al., 2016), due to its effectiveness in the removal of hydrophobic and humic-like substances.

Integrated membrane systems often use MF units prior to RO as a pretreatment to remove particles and bacteria. After MF, the

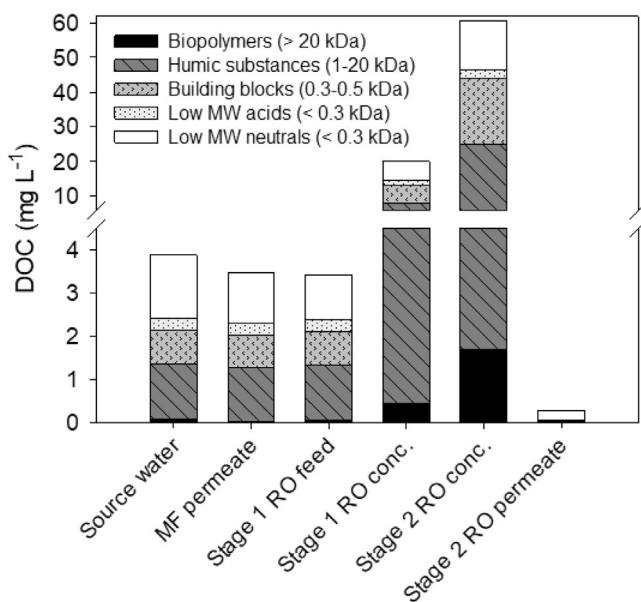


Fig. 2. The change of DOC composition in a full-scale integrated membrane system using liquid chromatography organic carbon detection (LC-OCD) ( $n = 7$ ).

concentrations of DOC, humic substances, building blocks, low-MW acids, and neutrals did not change significantly ( $p > 0.05$ ). The greatest significant reduction (51%) was observed in biopolymers ( $p < 0.05$ ), which mainly consisted of high-MW organic matter such as polysaccharides and macromolecular proteins. Biopolymers are also known to include extracellular polymers and soluble microbial products, which are major foulants of low-pressure membranes (e.g., MF and UF) (Nguyen et al., 2012). Therefore, pretreatments such as coagulation/sedimentation can be effective in minimizing membrane-fouling precursors. However, none of the EEM profiles, including the protein-like peak regions (T1 and T2) changed significantly after MF ( $p > 0.05$ ) (Fig. S1). This result suggest that the biopolymers rejected via MF were likely non-fluorescent polysaccharides, since these do not contribute to UV absorbance in the LC-OCD chromatogram (retention time between 20 and 40 min) (see Fig. S2).

The integrated membrane treatment plant introduces sodium bisulfate, phosphorus antiscalant, and CMIT/MIT to the stage 1 RO feed water basin (Fig. 1). The treatment caused only negligible changes in DOC composition and EEM intensities between the MF permeate and the stage 1 RO feed ( $p > 0.05$ ). Although the changes in NOM profiles were not significant, the average concentration of low-MW neutrals decreased by 12%, and that of biopolymers increased by 30% in the stage 1 RO feed basin. The low-MW neutrals could have been reduced via microbial utilization, since low-MW neutrals are known as a major source of AOC in membrane permeates (Meylan et al., 2007). This reduction was likely promoted by the phosphorus added as an antiscalant, since phosphorus can serve as an additional source of nutrients for the indigenous bacteria (Sweity et al., 2013). We can then suggest that observed increase in biopolymers may be related to the addition of antiscalants (of which a major component is organic polymers) or microbial products such as polysaccharides.

RO membrane treatment rejects most of the NOM but also generates waste concentrates that are rich in organics and inorganics (Ryu et al., 2016). In this study, the DOC concentration in the stage 1 RO concentrate increased to  $20 \text{ mg L}^{-1}$ , which was 6-fold higher than that of the feed water. The stage 1 RO concentrate consists of 2%, 38%, 26%, 7%, and 27% of biopolymers, humic substances, building blocks, low-MW acids, and low-MW neutrals, respectively (Fig. 2). The rates of increase of all EEM profiles were similar to that of the DOC concentration (5- or 6-fold increase) (Fig. S1) because of the rejection of dissolved NOM fluorophores and DOC.

As the stage 1 RO concentrate was sequentially fed to the stage 2 RO membranes, the DOC in the stage 2 RO concentrate increased significantly from 20 to  $59 \text{ mg L}^{-1}$  ( $p < 0.05$ ), while each of the EEM profiles also increased 3-fold. Interestingly, the relative abundances of low-MW acids and neutrals slightly decreased from 7% to 4% and from 26% to 23%, respectively, in stage 2 RO concentrate. Eventually, humic substances became predominant in the RO concentrates (39%). In contrast, Ryu et al. (2016) reported that the RO concentrate derived from WWTP effluent consisted mainly of building blocks followed by low-MW neutrals and acids; therefore, characteristics of RO membrane concentrates could differ per water sources and experimental conditions.

In the RO permeate, most of the DOC and the EEM intensities were significantly reduced ( $p < 0.05$ ), but  $0.2 \text{ mg L}^{-1}$  of low-MW neutrals was still detected (Fig. 2). Low-MW neutrals and acids unexpectedly passed through the RO membranes, and the low-MW neutrals were prevalent (81%) in DOC composition of the stage 2 RO permeate. According to Zhang et al. (2014), the DOC concentration of RO permeate depends on that of the feed water used. Moreover, low-MW organics could effectively pass through seawater RO membranes (Alshahri et al., 2017). Shan et al. (2009) reported that

low-MW neutrals could adsorb onto polyamide RO membranes and eventually pass through them. Generally, the industrial plants need ultrapure water which is often produced by RO process; therefore, remaining low-MW organics can be a problem.

### 3.2. Bacteriological characteristics in a full-scale integrated membrane system

Intact/damaged cell counts and bacterial ATP assays were carried out to determine the change of bacterial abundance and viability, respectively, in a full-scale integrated membrane system ( $n = 7$ ) (Fig. 3). Intact and damaged cell counts in the source water accounted for 37% and 63% of the total cell counts ( $9.6 \pm 2.5 \times 10^5$  cells  $\text{mL}^{-1}$ ), respectively. Bacterial ATP concentration of the source water was  $266 \pm 94$   $\text{ng L}^{-1}$ . The cell counts and bacterial ATP in the source water were relatively low compared with those of freshwater, as reported in our previous study ( $2 \times 10^6$  total cells  $\text{mL}^{-1}$  and  $600$   $\text{ng L}^{-1}$  bacterial ATP) (Park et al., 2016), likely owing to pretreatment of the source water.

In the MF permeate, 85% of the total cell count and 63% of bacterial ATP were dramatically excluded from the source water ( $p < 0.05$ ). However, bacterial passage through MF resulted in a relatively high residual cell count in the MF permeate of  $1.5 \pm 1.0 \times 10^5$  cells  $\text{mL}^{-1}$ . Ghayeni et al. (1999) has reported that the bacterial log removal via lab-scale MF membranes (i.e., using  $0.05$ ,  $0.2$ , and  $0.1 \mu\text{m}$  polycarbonate and  $0.22 \mu\text{m}$  polyvinylidene fluoride membranes) was considerably higher (i.e., up to 4) than that observed in our results from a full-scale MF (LRV = 0.8). The observed bacterial passage through full-scale MF membranes indicated that either the occurrence of membrane damage or the presence of the microfilterable form of bacteria in the feed water. External pressure also influences a reduction in bacterial cell volume. This volume reduction comes with the cell deformation, the magnitude of this process is determined by cell mechanical properties such as cell-wall flexibility. Thus, operational pressure can select for certain type of bacteria depending on their characteristics such as size, shape, surface charge but also the cell wall structure and flexibility (Lebleu et al., 2009). According to FCM measurement, the relative composition of HNA cells, which are relatively large and active (Wang et al., 2009; Hammes and Egli, 2010), was increased in full-scale MF permeate (Fig. S3). We initially expected that LNA bacteria, which have smaller biovolume, would be predominant in

all the MF permeates, but HNA bacteria were more abundant than LNA bacteria in the full-scale MF permeate. Considering that full-scale systems have many operational and environmental variables, the MF membrane units may have been damaged and thus allowed the passage of relatively large bacteria, unexpectedly. Hence, we suggest that FCM can be applied as a tool to detect failures in MF-based water treatment systems.

The stage 1 RO feed water contained sodium bisulfate, phosphorus antiscalant, and CMIT/MIT. Interestingly, the intact cell counts was not seen to differ significantly ( $p > 0.05$ ) in the stage 1 RO feed. In addition, no significant change in bacterial ATP was observed between the MF permeate and RO feed ( $p > 0.05$ ). This results suggest that the  $0.5$  ppm of CMIT/MIT did not effectively reduce the microbial activity. Different factors can be associated with the unexpectedly boost of bacterial growth in the RO feed water basin including the insufficient biocide, addition of phosphorus antiscalant, and the natural water constituents (i.e., bacterial abundance, their activity, and NOM substrates). All these factors could induce the development of biofilms or biofouling in the subsequent RO membranes and negatively influence their performance.

The total cell (intact + damaged cells) count in the stage 1 RO concentrate was 73% of that detected in the source water. A turnover of intact/damaged cells was also observed between the stage 1 RO feed and concentrates; the relative abundance of intact cells increased from 54% to 76%. Bacterial ATP increased to 9 times that of the stage 1 RO feed water. Total cell counts and bacterial ATP in the stage 2 RO concentrate were  $1.5 \pm 0.8 \times 10^6$  cells  $\text{mL}^{-1}$  and  $884 \pm 344$   $\text{ng L}^{-1}$ , respectively. Bacteria separated via RO membranes were still biologically active with respect to intact cell abundance (75%) and bacterial ATP (Fig. 3). CMIT/MIT biocides are often used to inhibit the ATP synthesis of microorganisms in various industrial applications (Williams, 2007), but the ATP detected in the RO concentrates showed that the biocide dosage used in this study was not effective in controlling biological growth. The use of biocides to control biological growth on membranes often results in biofilm formation and subsequent after growth activity (Al-Amoudi et al., 2007). Biofilms formed on membranes can be resistant to biocides and disinfectants and the production of EPS, extracellular polymeric matrix, acts as a reactive transport barrier to biocides (Matin et al., 2011). In the stage 2 RO permeate, the total cell count and bacterial ATP were present at levels near the detection limit, indicating that most of the bacteria had been rejected.

### 3.3. Passage of bacteria through a syringe MF filter and their growth potential

After observing the bacterial passage through full-scale MF units, we conducted lab-scale MF experiments in order to isolate microfilterable bacteria and compare the full-vs. lab-scale MF with the new and sterile membranes (e.g., syringe-driven filter). Because WWTP effluent is occasionally reused in RO membrane filtration, we also carried out the isolation of microfilterable bacteria derived from WWTP secondary effluent. Source water and WWTP effluent were filtered with a  $0.1 \mu\text{m}$  syringe-driven filter, and the indigenous bacteria in the MF permeates were cultivated as described in Wang et al. (2009).

Prior to filtration, the source water and WWTP effluent contained  $0.9 \times 10^6$  and  $4.0 \times 10^6$  cells  $\text{mL}^{-1}$  per total cell counts. The HNA/LNA bacterial compositions in the raw samples differed substantially; the bacterial abundance in the WWTP effluent mainly consisted of LNA bacteria (up to 75%) (Fig. 4), compared to that of source water (up to 33%). Bacterial abundance was relatively low in source water due to coagulation/sedimentation as a pretreatment.

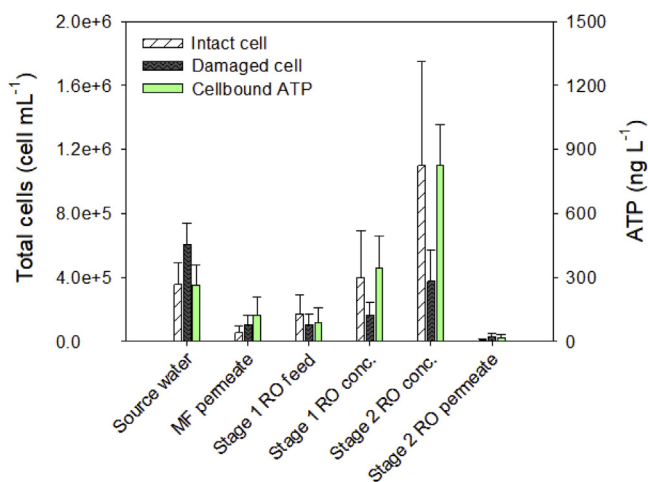
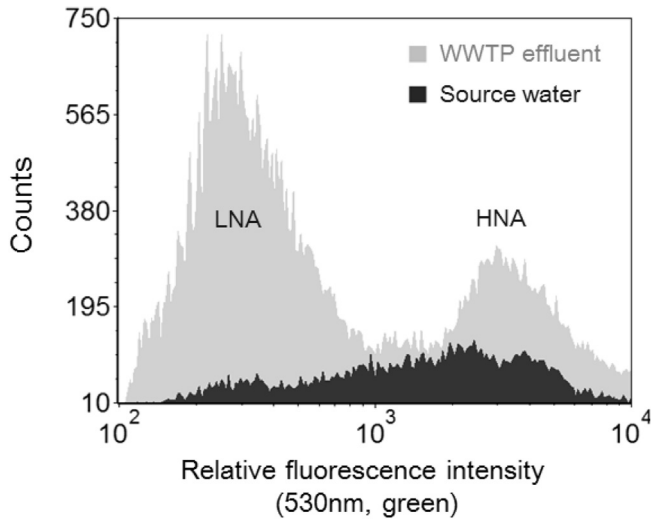


Fig. 3. The changes of intact/damaged cell count in a full-scale integrated membrane system. Error bars represent standard deviations ( $n = 7$ ). The  $p$  value obtained with one-way ANOVA among water samples was less than 0.05.



**Fig. 4.** The difference of flow cytometric histograms on HNA/LNA bacterial composition of total cells in the source water (black histogram) and wastewater treatment plant (WWTP) effluent (grey histogram), respectively. HNA and LNA bacteria were discriminated based on relative green fluorescence (530 nm) intensities. WWTP effluent was significantly rich in LNA bacteria compared to that of the source water.

LNA-bacteria richness in secondary effluent may be due to the morphology and activity of the microbiota in activated sludge. In this regard, wastewater reuse via membrane treatment may allow increased bacterial passage through MF owing to LNA-bacteria richness in the WWTP effluent. Initially,  $3.9 \times 10^4$  and  $2.3 \times 10^4$  cells  $\text{mL}^{-1}$  were detected in the MF permeates from the source water and WWTP effluent, respectively, as a result of bacterial passage through a syringe filter (Fig. 5). The number of LNA

bacteria that were able to pass through the filters was higher (72% and 92% for the isolates derived from source water and WWTP effluent, respectively) than that of HNA bacteria, possibly owing to their relatively small size and lower biovolume (Wang et al., 2008).

The filterable bacteria were cultivated at 30 °C for several days, and periodic samples were removed and analyzed to identify the bacterial composition during regrowth. HNA bacteria first increased and became predominant over LNA bacteria within 72 h in both samples (Fig. 5a and b). The changes in total ATP concentration correlated more closely to the growth of HNA bacteria ( $R^2 = 0.66$ ) than to that of LNA bacteria ( $R^2 = 0.27$ ). Most of the HNA bacteria can be efficiently rejected via MF, but they rapidly increased thereafter, owing to their relatively higher biological activity (e.g., productivity, esterase activity, and ATP-per-cell count) (Vital et al., 2012; Park et al., 2016), regardless of their initial cell density (Fig. 5).

### 3.4. Growth potentials of filterable bacteria in a full-scale integrated membrane system

Bacterial growth is often limited by assimilable organic substrate and available nutrients in a water sample (Prest et al., 2016). To determine the growth ability of filterable bacteria in water samples, we performed a growth potential assay, modified from Vital et al. (2010) that simulated bacterial growth of specific inocula (e.g., pathogenic bacteria) interacting with AOC in a full-scale water treatment process. Therefore, bacteria isolated from lab-scale MF permeates were used as inocula to simulate the growth potential of filterable bacteria in a full-scale membrane system. Fig. 6 shows the changes in growth potentials for filterable bacteria derived from two different origins (i.e., source water and WWTP effluent). In the source water, the growth potentials of filterable bacteria derived from the source water (SW) and WWTP effluent (WW) were  $7.2 \pm 2.7 \times 10^5$  and  $5.4 \pm 2.0 \times 10^5$  cells  $\text{mL}^{-1}$ , respectively (Fig. 6).

In the MF permeate, the grown cell counts of filterable bacteria SW and WW significantly decreased by 64% and 48%, respectively ( $p < 0.05$ ). Since no significant change was observed in MF

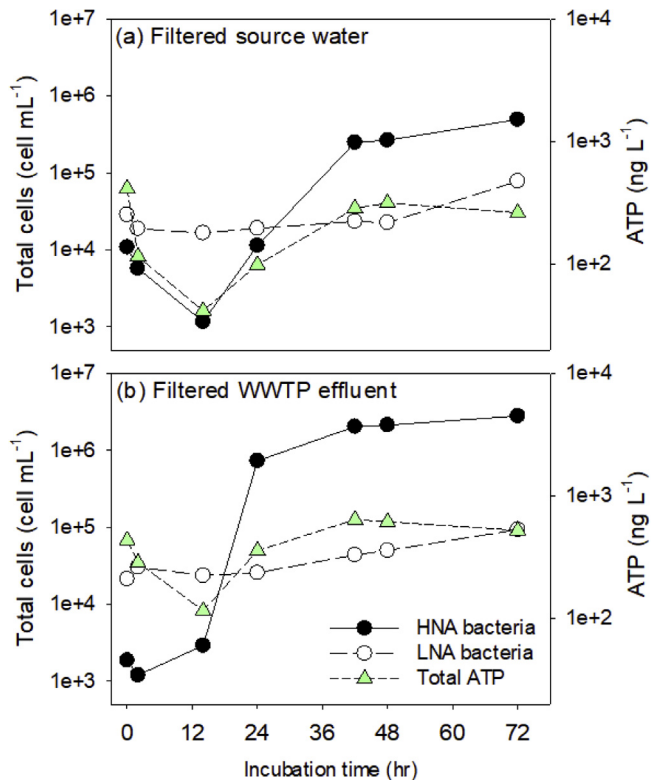


**Fig. 5.** The regrowth of filterable bacteria after filtration of the source water (a) and WWTP effluent (b) with 0.1  $\mu\text{m}$  syringe-driven filter.

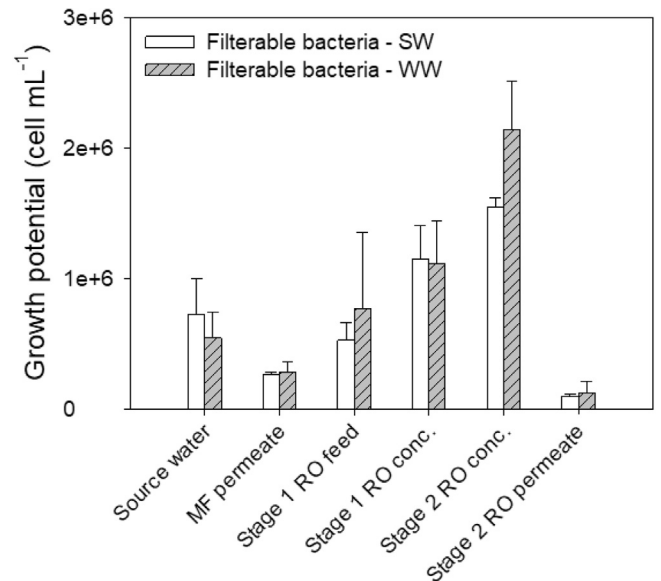


**Fig. 6.** Comparison of the growth potentials in each treatment step of an integrated membrane system, individually inoculated with filterable bacteria from the source water (SW) and WWTP effluent (WW). The error bars represent standard deviations ( $n = 4$ ). The  $p$  value obtained with one-way ANOVA among water samples was less than 0.05.

permeate NOM composition except for biopolymers ( $p < 0.05$ ) (Fig. 2), this decrease in MF permeate growth potential is likely due to MF-mediated removal of approximately half of the AOC, which consists of high-MW fractions such as biopolymers, from the source water (Elhadidy et al., 2016; Park et al., 2016).

In the stage 1 RO feed water, the growth potential increased by 2–3 times compared to that of the MF permeate despite their similar DOC compositions (Fig. 2). This difference could be due to the introduction of chemicals, such as the phosphorus-based antiscalant and sodium bisulfate, in the stage 1 RO feed water. Several studies have reported that phosphorus antiscalants can increase nutrients and substrates in RO feed water (Sweity et al., 2013; Vrouwenvelder et al., 2010); therefore, non-phosphorus antiscalants have recently been increasingly applied. Hence, we conducted an additional test on the effects of the phosphorus antiscalant at the same time as the growth potential test. Addition of 1 ppm of phosphorus antiscalant, equal to the amount used in the full-scale system, promoted a 10% increase in bacterial growth compared to a full-scale MF permeate with no antiscalant for control (Fig. S4). In addition, chlorination is used after pretreatment in the source water, but the subsequent dichlorination can also cause rapid microbial growth and biofilm development on RO membranes (Saeed et al., 2000). Therefore, replacing the chemicals used can reduce the increase in bacterial growth potential of the RO feed water.

In the RO concentrates, the growth potentials increased in association with the accumulation of DOC (Figs. 2 and 6). The growth potentials in the stage 1 RO concentrates of filterable bacteria collected from source water and WWTP effluent increased by 2.2 and 1.5 times, respectively, and those of the stage 2 RO concentrates by 1.4 and 1.9 times, respectively. Despite the high NOM concentrations ( $\text{DOC} > 20 \text{ mg L}^{-1}$ ) of the RO concentrates, the AOC concentrations in both RO concentrates were relatively low (i.e., equivalent to 3–6  $\mu\text{g mg}^{-1}$  AOC/DOC per sample) compared to reported assimilable organic compositions in natural freshwaters

(i.e., higher than 16  $\mu\text{g mg}^{-1}$  AOC/DOC) (Gasol et al., 1999; Volk and LeChevallier, 2000). The growth potential in the RO permeate was very low, corresponding to the negligible DOC concentration in this water sample (Fig. 2). We can conclude that the stage 2 RO permeate water may be more biologically stable in comparison with other samples because most of the available organics and nutrients will be removed after RO membrane filtration. Biological stability refers to the concept that water preserves the same microbial quality and normally to achieve this limit bacterial growth occurs during transport and treatments (Prest et al., 2016). Thus, it is possible to hypothesise that if the available organics and nutrients are removed bacterial growth will be limited and controlled.

### 3.5. Changes in bacterial communities via MF and RO

The bacterial community structures of the source water, membrane permeates, and an autopsied RO biofilm was investigated in order to determine the bacterial taxa that can pass through the lab- and full-scale MF membranes. We collected the mature biofilm formed on the surface of an end-of-life RO membrane (Fig. S5) in order to understand the effect of MF bacterial passage on resultant RO biofilm community structures. The 16s rRNA sequencing technique was used to reveal the bacteria community structures from each origin (i.e., source water and WWTP effluent) that was applied to the growth potential tests as well as in the different treatment effluents and the eventual RO biofilm.

Sequencing results shown that *Proteobacteria*, *Bacteroidetes*, and *Actinobacteria* were the most predominant phyla in all the samples analyzed (92–99% per sample) (data not shown). *Proteobacteria* was the dominant phylum in all samples (57–98% per sample), except for the RO biofilm where *Bacteroidetes* represented 50% of the total microbial community structure. In the source water, the bacteria mainly belonged to the class *Alphaproteobacteria* (42%) followed by *Flavobacteria*, *Betaproteobacteria*, *Sphingobacteria*, and *Actinobacteria*. At the family level, *Sphingomonadaceae* (27%) was

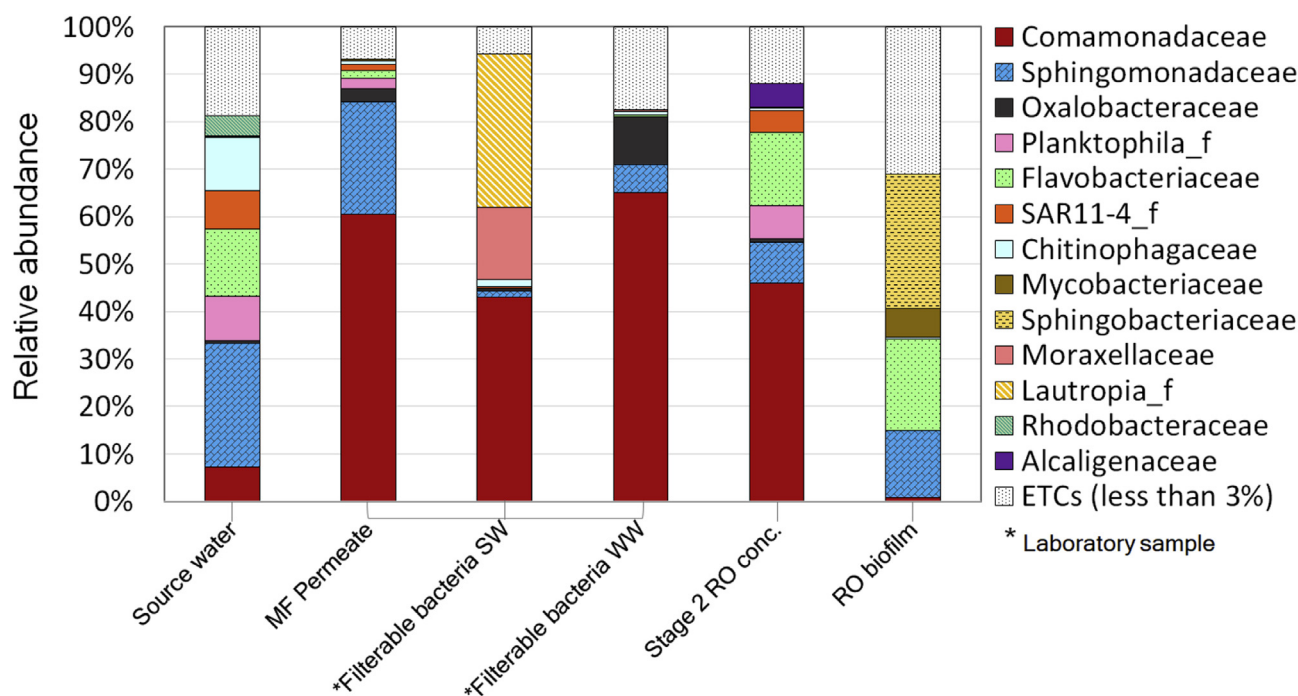
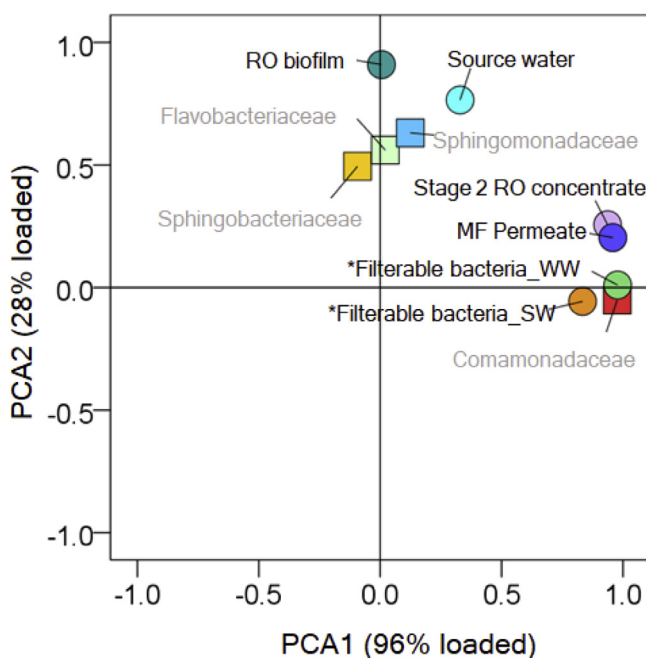


Fig. 7. The bacterial community structures in source water, treatment effluents, and RO biofilm (family-level). In particular, bacterial community in full-scale MF permeate was compared with \*laboratory samples: the filterable bacteria derived from the source water (SW) and wastewater effluent (WW). The full-scale stage 2 RO concentrate was also analyzed due to its high cell density. In contrast, the analysis of RO permeate that have low cell density was neglected.

followed by *Flavobacteriaceae* (15%), *Chitinophagaceae* (12%) (Fig. 7). Notably, the bacterial communities changed dramatically in the MF permeate. *Betaproteobacteria* became the predominant class in the total bacterial populations of the MF permeate (65%). Within *Betaproteobacteria*, *Comamonadaceae*, followed by *Sphingomonadaceae* and *Oxalobacteraceae* were the main represented subdivisions (Fig. 7). Interestingly, the laboratory bacterial samples we isolated via syringe-driven filtration (i.e., filterable bacteria derived from the source water and WWTP effluent) also consisted mainly of *Comamonadaceae*. Overall, *Comamonadaceae* accounted for approximately half of the sequences in the microbial communities of the full-scale MF permeate, RO concentrate, and two laboratory bacterial isolates (filterable bacteria SW and WW) (Fig. 7). *Comamonadaceae* are common inhabitants of oligotrophic environments and have been observed as important components of the microbial community structure also in sand filters in drinking water plants (Vandermaesen et al., 2017) and in sediments of drinking water storage tanks (Qin et al., 2017). In contrast, *Comamonadaceae* accounted for only 1% of the RO biofilm community. The *Sphingobacteriaceae* subdivision was the most prevalent in the RO biofilm community (28%), followed by *Flavobacteriaceae* (19%), *Sphingomonadaceae* (14%), and *Mycobacteriaceae* (6%) (Fig. 7). Microbial diversity at the species level in the RO biofilm was relatively high ( $H' = 4.3$ ) compared to that of the MF-treated water ( $H'$  range: 2.2–3.8 per sample), but it was equivalent to that of the source water ( $H' = 4.1$ ).

PCA analysis of the bacterial community structure at family level (Fig. 8) shows relative distances between environmental samples with respect to water constituents such as organics, inorganics, and the microbiome. According to the PCA plotting, the bacterial community of the RO biofilm was relatively similar to that of the source water and was associated to the presence of *Sphingomonadaceae*, *Flavobacteriaceae*, and *Sphingobacteriaceae*. The MF-treated water and filterable bacteria samples tended to group together with the family *Comamonadaceae*, but not a clear relationship was observed



**Fig. 8.** Principal component analysis describing the relationships of the bacterial community structures in source water, treatment effluents, \*laboratory samples, and RO biofilm (family-level). Circles represent the bacterial community characters of each samples (Fig. 7) whereas squares represent idealized pure bacterial families (100%, grey text).

between the filterable bacteria and RO biofilm community. Accordingly, most of the *Comamonadaceae* that passed through MF did not take part in the RO biofilm community, but the filterable forms of *Flavobacteriaceae* and *Sphingomonadaceae* did contribute to the RO biofilm. These results confirm that *Comamonadaceae* were the main bacterial group determining the community structure of filterable bacteria while RO biofilms were selective habitats where other microbial families tended to accumulate. *Comamonadaceae* are often associated with biological instability of treated water that has readily available substrates to induce unexpected biofilm formation (Gao et al., 2013; Proctor et al., 2016); therefore, the richness in *Comamonadaceae* can be related to the bacterial regrowth in the MF-treated effluents. Previous studies also reported that filterable microbes (e.g., *Hydrogenophaga*, *Hylemonella*, *Curvibacter* and others) often belonged to the family *Comamonadaceae* (Wang et al., 2008; Lee et al., 2010; Fedotova et al., 2012). These studies interestingly pointed out that the filterable *Comamonadaceae* had short and narrow cells (0.1–0.3  $\mu\text{m}$ -width curved-rod or spirilla). Moreover, bacteria, living under oligotrophic conditions, could be observed to reduce their size compared to that in richer growth medium conditions (0.3–0.5  $\mu\text{m}$ -width). In the present study, the filterable *Comamonadaceae* sequences mainly belonged to the genera *Hydrogenophaga*, *Curvibacter* and *Limnohabitans*, often found in oligotrophic environments (Vandermaesen et al., 2017); therefore, bacterial passage, observed in both lab- and full-scale MF tests in this study, can be related with their cell shape and nutrient conditions in source water.

The families *Flavobacteriaceae*, *Sphingobacteriaceae* and *Sphingomonadaceae* have often been found in mature RO biofilm communities (Bereschenko et al., 2007, 2008; 2010; Barnes et al., 2015), but other studies have reported that *Betaproteobacteria* can also be found in young biofilms (Bereschenko et al., 2010; Barnes et al., 2015). Therefore, the filterable bacteria may play a role in seeding the initial RO biofilm development. In addition, Bereschenko et al. (2010) revealed that *Betaproteobacteria* can often colonize the outer layers of mature biofilms, forming an outer microbial community that can be vulnerable to membrane cleaning schemes (Bereschenko et al., 2011; Barnes et al., 2015). Therefore, how RO membranes are managed may also affect the specific bacterial composition of a RO biofilm. In summary, whereas the bacterial taxa that passed through MF likely played a role in seeding the RO biofilm, several key biofouling players, such as *Flavobacteriaceae*, *Sphingobacteriaceae* and *Sphingomonadaceae*, can be selectively incorporated into the final mature RO biofilm community structure.

#### 4. Conclusions

This study provides a better understanding of microfilterable bacteria in integrated membrane treatment systems where biofouling is a critical problem. Our results revealed the effects of bacterial passage through MF versus RO membranes in a full-scale industrial water treatment plant. The bacterial removal rates via MF reported in previous studies may have been underestimated compared to that of full-scale study. Our extensive analysis revealed that bacterial passage occurs in all MF permeates regardless of full- and lab-scale MF treatments. Because the complete rejection of environmental bacteria and biodegradable NOM cannot be guaranteed through the use of MF membranes, bacteria that passes through MF are able to continuously utilize substrates and reproduce thereafter in integrated membrane systems with RO membranes. Changes in NOM composition during the course of water treatment resulted in variation in the growth potentials of filterable bacteria, which are important factors in the occurrence of biofilms on RO membranes. Chemicals used in integrated membrane systems were also seen to affect the growth potentials of

bacteria. The use of phosphorus RO membrane antiscalants can boost bacterial growth if the raw water contains microfilterable bacteria. Notably, the taxa of filterable bacteria, which mainly consists of the family *Comamonadaceae*, may act as the initial seeds of RO biofilms; however, mature RO biofilms are often colonized by several biofouling players, including *Flavobacteriaceae*, *Sphingobacteriaceae* and *Sphingomonadaceae*. Therefore, biofilm monitoring and control strategies should target these specific microbial members to avoid adverse biofouling processes that can affect the final quality of the water.

## Acknowledgments

This research was supported by the Basic Science Research Program through the National Research Foundation of Korea (NRF) funded by the Ministry of Science, ICT and Future Planning, Republic of Korea [Grant number: 2017R1A1A1A05001231]. We would like to thank Prof. Boxall from the Department of Civil and Structural Engineering, The University of Sheffield for giving us the opportunity to work with Dr. Douterelo in this study through the framework of international cooperation program managed by National Research Foundation of Korea.

## Appendix A. Supplementary data

Supplementary data related to this article can be found at <https://doi.org/10.1016/j.watres.2018.07.027>.

## References

- Al-Amoudi, A., Lovitt, R.W., 2007. Fouling strategies and the cleaning system of NF membranes and factors affecting cleaning efficiency. *J. Membr. Sci.* 303 (1–2), 6–28.
- Alshahri, A.H., Dehwah, A.H.A., Leiknes, T., Missimer, T.M., 2017. Organic carbon movement through two SWRO facilities from source water to pretreatment to product with relevance to membrane biofouling. *Desalination* 407, 52–60.
- Barnes, R.J., Low, J.H., Bandi, R.R., Tay, M., Chua, F., Aung, T., Fane, A.G., Kjelleberg, S., Rice, S.A., 2015. Nitric oxide treatment for the control of reverse osmosis membrane biofouling. *Appl. Environ. Microbiol.* 81 (7), 2515–2524.
- Bereschenko, L.A., Heilig, G.H.J., Nederlof, M.M., Van Loosdrecht, M.C.M., Stams, A.J.M., Euverink, G.J.W., 2008. Molecular characterization of the bacterial communities in the different compartments of a full-scale reverse-osmosis water purification plant. *Appl. Environ. Microbiol.* 74 (17), 5297–5304.
- Bereschenko, L.A., Prummel, H., Euverink, G.J.W., Stams, A.J.M., van Loosdrecht, M.C.M., 2011. Effect of conventional chemical treatment on the microbial population in a biofouling layer of reverse osmosis systems. *Water Res.* 45 (2), 405–416.
- Bereschenko, L.A., Stams, A.J.M., Euverink, G.J.W., van Loosdrecht, M.C.M., 2010. Biofilm formation on reverse osmosis membranes is initiated and dominated by sphingomonas spp. *Appl. Environ. Microbiol.* 76 (8), 2623–2632.
- Bereschenko, L.A., Stams, A.J.M., Heilig, G.H.J., Euverink, G.J.W., Nederlof, M.M., Van Loosdrecht, M.C.M., 2007. Investigation of microbial communities on reverse osmosis membranes used for process water production. *Water Sci. Technol.* 55 (8–9), 181–190.
- Berney, M., Vital, M., Hulshoff, I., Weilenmann, H.U., Egli, T., Hammes, F., 2008. Rapid, cultivation-independent assessment of microbial viability in drinking water. *Water Res.* 42 (14), 4010–4018.
- Elhadidy, A.M., Van Dyke, M.J., Peldszus, S., Huck, P.M., 2016. Application of flow cytometry to monitor assimilable organic carbon (AOC) and microbial community changes in water. *J. Microbiol. Meth.* 130, 154–163.
- Escobar, I.C., Randall, A.A., 2001. Assimilable organic carbon (AOC) and biodegradable dissolved organic carbon (BDOC): complementary measurements. *Water Res.* 35 (18), 4444–4454.
- Fedotova, A.V., Belova, S.E., Kulichevskaya, I.S., Dedysh, S.N., 2012. Molecular identification of filterable bacteria and archaea in the water of acidic lakes of northern Russia. *Microbiology* 81 (3), 281–287.
- Gao, D.W., Fu, Y., Ren, N.Q., 2013. Tracing biofouling to the structure of the microbial community and its metabolic products: a study of the three-stage MBR process. *Water Res.* 47 (17), 6680–6690.
- Gasol, J.M., Zweifel, U.L., Peters, F., Fuhrman, J.A., Hagstrom, A., 1999. Significance of size and nucleic acid content heterogeneity as measured by flow cytometry in natural planktonic bacteria. *Appl. Environ. Microbiol.* 65 (10), 4475–4483.
- Ghayeni, S.B.S., Beatson, P.J., Fane, A.J., Schneider, R.P., 1999. Bacterial passage through microfiltration membranes in wastewater applications. *J. Membr. Sci.* 153 (1), 71–82.
- Hammes, F., Egli, T., 2010. Cytometric methods for measuring bacteria in water: advantages, pitfalls and applications. *Anal. Bioanal. Chem.* 397 (3), 1083–1095.
- Herzberg, M., Berry, D., Raskin, L., 2010. Impact of microfiltration treatment of secondary wastewater effluent on biofouling of reverse osmosis membranes. *Water Res.* 44 (1), 167–176.
- Hijnen, W.A.M., Biraud, D., Cornelissen, E.R., van der Kooij, D., 2009. Threshold concentration of easily assimilable organic carbon in feedwater for biofouling of spiral-wound membranes. *Environ. Sci. Technol.* 43 (13), 4890–4895.
- Huber, S.A., Balz, A., Abert, M., Pronk, W., 2011. Characterisation of aquatic humic and non-humic matter with size-exclusion chromatography - organic carbon detection - organic nitrogen detection (LC-OCD-OND). *Water Res.* 45 (2), 879–885.
- Lebleu, N., Roques, C., Aïmar, P., Causserand, C., 2009. Role of the cell-wall structure in the retention of bacteria by microfiltration membranes. *J. Membr. Sci.* 326 (1), 178–185.
- Lee, A., Mcvey, J., Faustino, P., Lute, S., Sweeney, N., Pawar, V., Khan, M., Brorson, K., Hussong, D., 2010. Use of *Hydrogenophaga pseudoflava* penetration to quantitatively assess the impact of filtration parameters for 0.2-micrometer-pore-size filters. *Appl. Environ. Microbiol.* 76 (3), 695–700.
- Li, C., Yang, Y., Ding, S.Y., Hou, L.A., 2016. Dynamics of biofouling development on the conditioned membrane and its relationship with membrane performance. *J. Membr. Sci.* 514, 264–273.
- Lillis, T.O., Bissonnette, G.K., 2001. Detection and characterization of filterable heterotrophic bacteria from rural groundwater supplies. *Letts. Appl. Microbiol.* 32 (4), 268–272.
- Mannik, J., Driessen, R., Galajda, P., Keymer, J.E., Dekker, C., 2009. Bacterial growth and motility in sub-micron constrictions. *Proc. Natl. Acad. Sci. U.S.A.* 106 (35), 14861–14866.
- Matin, A., Khan, Z., Zaidi, S.M.J., Boyce, M.C., 2011. Biofouling in reverse osmosis membranes for seawater desalination: phenomena and prevention. *Desalination* 281, 1–16.
- Meylan, S., Hammes, F., Traber, J., Salhi, E., von Gunten, U., Pronk, W., 2007. Permeability of low molecular weight organics through nanofiltration membranes. *Water Res.* 41 (17), 3968–3976.
- Nguyen, T., Roddick, F.A., Fan, L., 2012. Biofouling of water treatment membranes: a review of the underlying causes, monitoring techniques and control measures. *Membranes* 2 (4), 804–840.
- Onyango, L.A., Dunstan, R.H., Roberts, T.K., 2010. Filterability of staphylococcal species through membrane filters following application of stressors. *BMC Res. Notes* 3, 152.
- Park, J.W., Kim, H.C., Meyer, A.S., Kim, S., Maeng, S.K., 2016. Influences of NOM composition and bacteriological characteristics on biological stability in a full-scale drinking water treatment plant. *Chemosphere* 160, 189–198.
- Prest, E.I., Hammes, F., van Loosdrecht, M.C.M., Vrouwenvelder, J.S., 2016. Biological stability of drinking water: controlling factors, methods, and challenges. *Front. Microbiol.* 7.
- Proctor, C.R., Gachter, M., Kotsch, S., Rolli, F., Sigrist, R., Walser, J.C., Hammes, F., 2016. Biofilms in shower hoses - choice of pipe material influences bacterial growth and communities. *Environ. Sci. Water Res. Technol.* 2 (4), 670–682.
- Qin, K., Struewing, I., Domingo, J.S., Lytle, D., Lu, J., 2017. Opportunistic pathogens and microbial communities and their associations with sediment physical parameters in drinking water storage tank sediments. *Pathogens* 6 (4).
- Ryu, J., Jung, J., Yu, Y., Kweon, J., 2016. Evaluation of organic matter characteristics of FO and RO concentrates. *Desalination Water Treat.* 57 (1), 24606–24614.
- Sack, E.L., van der Wielen, P.W., van der Kooij, D., 2014. Polysaccharides and proteins added to flowing drinking water at microgram-per-liter levels promote the formation of biofilms predominated by bacteroidetes and proteobacteria. *Appl. Environ. Microbiol.* 80 (8), 2360–2371.
- Saeed, M.O., Jamaluddin, A.T., Tisan, I.A., Lawrence, D.A., Al-Amri, M.M., Chida, K., 2000. Biofouling in a seawater reverse osmosis plant on the Red Sea coast, Saudi Arabia. *Desalination* 128 (2), 177–190.
- Shan, J.H.H., J. Y. Ong, S.L., 2009. Adsorption of neutral organic fractions in reclaimed water on RO/NF membrane. *Separ. Purif. Technol.* 67, 1–7.
- Shannon, C.E., 1997. The mathematical theory of communication (Reprinted). *M D Computing*, 14 (4), 306–317.
- Sweity, A., Oren, Y., Ronen, Z., Herzberg, M., 2013. The influence of antiscalants on biofouling of RO membranes in seawater desalination. *Water Res.* 47 (10), 3389–3398.
- Vandermaesen, J., Lievens, B., Springael, D., 2017. Isolation and identification of culturable bacteria, capable of heterotrophic growth, from rapid sand filters of drinking water treatment plants. *Res. Microbiol.* 168 (6), 594–607.
- Vital, M., Dignum, M., Magic-Knezeu, A., Ross, P., Rietveld, L., Hammes, F., 2012. Flow cytometry and adenosine tri-phosphate analysis: alternative possibilities to evaluate major bacteriological changes in drinking water treatment and distribution systems. *Water Res.* 46 (15), 4665–4676.
- Vital, M., Stucki, D., Egli, T., Hammes, F., 2010. Evaluating the growth potential of pathogenic bacteria in water. *Appl. Environ. Microbiol.* 76 (19), 6477–6484.
- Volk, C.J., LeChevallier, M.W., 2000. Assessing biodegradable organic matter. *J. AWWA (Am. Water Works Assoc.)* 92 (5), 64–76.
- Vrouwenvelder, J.S., Beyer, F., Dahmani, K., Hasan, N., Galjaard, G., Kruithof, J.C., van

- Loosdrecht, M.C.M., 2010. Phosphate limitation to control biofouling. *Water Res.* 44 (11), 3454–3466.
- Wang, Y.Y., Hammes, F., Boon, N., Chami, M., Egli, T., 2009. Isolation and characterization of low nucleic acid (LNA)-content bacteria. *ISME J.* 3 (8), 889–902.
- Wang, Y.Y., Hammes, F., Duggelin, M., Egli, T., 2008. Influence of size, shape, and flexibility on bacterial passage through micropore membrane filters. *Environ. Sci. Technol.* 42 (17), 6749–6754.
- Weinrich, L.A., Schneider, O.D., LeChevallier, M.W., 2011. Bioluminescence-based method for measuring assimilable organic carbon in pretreatment water for reverse osmosis membrane desalination. *Appl. Environ. Microbiol.* 77 (3), 1148–1150.
- Williams, T.M., 2007. The mechanism of action of isothiazolone biocides. *Power-Plant Chem* 9, 14–22.
- Zhang, Y., Huang, W., Ran, Y., Mao, J., 2014. Compositions and constituents of freshwater dissolved organic matter isolated by reverse osmosis. *Mar. Pollut. Bull.* 85 (1), 60–66.